ARTICLE
Journal of Cellular Biochemistry 116:2166–2176 (2015)

Journal of Cellular Biochemistry

MicroRNA-150 Protects Against Pressure Overload-Induced Cardiac Hypertrophy

Wanli Liu,[1,2] Yu Liu,[1,2] Yan Zhang,[1,2] Xueyong Zhu,[1,2] Rui Zhang,[1,2] Lihua Guan,[1,2] Qizhu Tang,[1,2] Hong Jiang,[1,2] Congxin Huang,[1,2] and He Huang[1,2]*

[1]*Department of Cardiology, Renmin Hospital of Wuhan University, Wuhan 430060, China*
[2]*Cardiovascular Research Institute, Wuhan University, Wuhan 430060, China*

ABSTRACT

Cardiac hypertrophy is the response of the heart to a variety of hypertrophic stimuli; this condition progresses to heart failure and sudden death. MicroRNAs (miRs) are a family of small, non-coding RNAs that mediate posttranscriptional gene silencing. Recent studies have identified miRs as important regulators in cardiac hypertrophy. One specific miR, miR-150 has been reported to be downregulated in hypertrophic murine hearts. However, the role of miR-150 as a regulator of cardiac hypertrophy remains unclear. In the present study, we used gain-of-function and loss-of-function approaches to investigate the functional roles of miR-150 in cardiac hypertrophy induced by aortic banding. The extent of the cardiac hypertrophy was evaluated by echocardiography and by pathological and molecular analyses of heart samples. Our results revealed that transgenic mice that overexpress miR-150 in the heart were resistant to cardiac hypertrophy and fibrosis through down-regulation of serum response factor (SRF). Conversely, the loss of function of miR-150 by genetic knockdown or antagomiR approaches produced the opposite effects. These studies suggest that miR-150 plays an important role in the regulation of cardiac hypertrophy and SRF is involved in miR-150 mediated anti-hypertrophic effect. Thus, miR-150 may be a new therapeutic target for cardiac hypertrophy. J. Cell. Biochem. 116: 2166–2176, 2015.

KEY WORDS: MICRORNA; HYPERTROPHY; SIGNAL TRANSDUCTION; SRF

Cardiac hypertrophy is a physiological and compensatory response to increased workload that is characterized by an increase in myocardial mass and the accumulation of extracellular matrix [Li et al., 2010; Zong et al., 2013]. In the general population, pathological cardiac hypertrophy is frequently associated with a poor clinical prognosis, including the development of cardiac systolic and diastolic dysfunction, arrhythmias, and the progression to heart failure as well as sudden death [Lorell and Carabello, 2000; Ruilope and Schmieder, 2008]. Despite extensive research over the past several decades, the exact molecular mechanisms that regulate gene expression during cardiac hypertrophy remain unclear.

MicroRNAs (miRs) are a novel class of ≈22-nucleotide endogenous non-protein-coding single-stranded RNAs that have recently garnered significant attention. These small molecules exert their regulatory effects by binding directly to target messenger RNAs (mRNAs) and affecting mRNA stability and translation [Jing et al., 2005; Wu et al., 2006]. Recent studies have demonstrated that miRs regulate many aspects of the cardiac pathological process including ischemia, reperfusion injury, hypertrophy, heart failure, and arrhythmia, suggesting that there is great potential for the development of miR-based therapeutic strategies for cardiovascular diseases [Yang et al., 2007; Lin et al., 2009; Wang et al., 2010; Montgomery et al., 2011; Aurora et al., 2012]. A recent review indicates that more than 10 miRs actively participate in the development of cardiac hypertrophy through distinct mechanisms [Da Costa Martins and De Windt, 2012]. However, as the cellular mechanisms underlying cardiac hypertrophy involve complex signaling molecules and pathways, the network of miRs that govern

Wanli Liu and Yu Liu are co-first authors.
Conflicts of interest: The authors have declared that no conflict of interest exists.
Grant sponsor: National Key Basic Research Development Program of China; Grant number: 2012CB518604; Grant sponsor: National Science and Technology Support Program of China; Grant number: 2011BAI11B12; Grant sponsor: National Natural Science Foundation of China; Grant numbers: 81100129, 81070142, 81270249.
*Correspondence to: He Huang, MD, PhD, Department of Cardiology, Renmin Hospital of Wuhan University, Cardiovascular Research Institute, Wuhan University, Jiefang Road 238, Wuhan 430060, PR China.
E-mail: huangwhu2011@163.com
Manuscript Received: 26 June 2014; Manuscript Accepted: 18 December 2014
Accepted manuscript online in Wiley Online Library (wileyonlinelibrary.com): 5 January 2015
DOI 10.1002/jcb.25057 • © 2015 Wiley Periodicals, Inc.

cardiac hypertrophy is highly complex. Therefore, it is important to understand the role of each dysregulated miR in cardiac hypertrophy.

One specific miR, miR-150, was initially identified as one of the deregulated miRs in primary chronic lymphocytic leukemia cells [Fulci et al., 2007]. This molecule has been reported to play a role in regulating the development of immune cells, oncogenesis, inflammation, and apoptosis [Xiao et al., 2007; Zhou et al., 2008; Vasilescu et al., 2009; Watanabe et al., 2011]. In the heart, microarray analysis of miRs revealed that miR-150 is downregulated in both thoracic aortic banding-induced and calcineurin A overexpression-induced cardiac hypertrophy, suggesting that miR-150 plays an important role in cardiac hypertrophy [van Rooij et al., 2006; Sayed et al., 2007]. However, the function and underlying mechanisms of miR-150 in the development of cardiac hypertrophy have not been investigated. In the present study, we demonstrate for the first time that cardiac-specific overexpression of miR-150 protects the heart against cardiac hypertrophy. Conversely, the knockdown or inhibition of endogenous miR-150 promotes cardiac hypertrophy. Our findings indicate that miR-150 is a critical modulator in the development of cardiac hypertrophy.

MATERIALS AND METHODS

ANIMALS AND ANIMAL MODELS

All of the animal investigations were performed in accordance with the approval of our Renmin Hospital of Wuhan University Animal Care and Use Committee. Male wild type C57BL/6 mice and miR-150 knockout mice were purchased from Beijing HFK Bioscience Co. Ltd. and the Jackson Laboratory, respectively. MiR-150 transgenic mice that overexpress human miR-150 were created by our laboratory. All of the mice were used for experiments at 8–10 weeks of age. The mice were lightly anesthetized with pentobarbital (peritoneal injection) and aortic banding (AB) was performed. A sterna split was performed, and a 7–0 silk ligature was tied around the ascending aorta and a 26 G (for mice with a weight of 25.0–27.5 g) or 27 G (for mice with a weight of 23.5–25.0 g) blunted needle, which was subsequently removed. Sham-operated animals underwent the same procedure without the banding of the aorta. After the operation, the animals were returned to their cages for an additional 4 weeks (knockout mice and mini pump mice) or 8 weeks (transgenic mice). At 2 weeks after the operation, osmotic mini pumps (model 2002, Alzet), which were prepared and placed in 0.9% saline at 37°C for approximately 48 h to ensure continuous delivery of the drug, were inserted subcutaneously between the shoulder blades to deliver antagomiR at a dose of 15 mg/kg body weight for 2 weeks.

ECHOCARDIOGRAPHY

Echocardiograph examinations were performed under standardized conditions with the animals in the supine position, spontaneously breathing on a mask though the trachea using 2% isoflurane and 98% O_2. The echocardiographic data were analyzed using the average of three representative cycles by MyLab 30 (Esaote). Two-dimensional (2D) images of the LV were obtained in both long and short axes, which were obtained at the level of the papillary muscle. M-mode tracings were recorded at the level of both the papillary muscles and the aortic valves using 2D guidance. The LV cavity dimensions were measured through the largest diameter of the ventricle in both systole and diastole. The percentage LV fractional shortening (LVFS) was calculated using the following formula: $LVFS = (LVEDD - LVESD)/LVEDD \times 100$. Doppler recordings were obtained in the left parasternal long axis position.

HISTOLOGICAL ANALYSIS

The mice were killed by decapitation after experimentation. The hearts and lungs were then removed and blotted free of blood immediately, weighed, and normalized to the body weight (HW/BW and LW/BW) and tibia length (HW/TL). The atria and right ventricles of several hearts were cut away, and the left ventricular tissue was frozen in liquid nitrogen and stored at −80°C for biochemical analysis. The other hearts, which were post-fixed in formaldehyde solution, were processed into paraffin wax for morphometric analysis. Five-micrometer-thick transverse (short-axis) slices of the heart at the level of the papillary muscles were analyzed from each tissue sample. The sections were stained using hematoxylin-eosin (HE) for morphology and assessing the myocardial area. Picrosirius red (PSR) staining was used to assess the extent of myocardial collagen deposition. The red (collagen) staining was normalized against the yellow (cardiomyocyte) staining for each heart. Morphometric analysis was performed using the image analysis program Image-Pro Plus (version6.0).

CULTURED H9C2 CELLS AND IN VITRO HYPERTROPHY ASSAYS

H9C2 cells were cultured in 6-well plates at a density of 10^6 cells/ml in DMEM supplemented with 10% fetal calf serum and maintained in a 37°C, 5% CO_2 incubator. The cells were transfected with the miR-150 mimic, mimic control, antagomiR-150, or antagomiR control (GenePharma Co., Ltd, Shanghai, China) using Lipofectamine 2000 (Invitrogen), according to the manufacturer's instructions, at a final concentration of 50 nM for 24 h prior to AngII or PBS administration. The cells were harvested after 12 h, at which time point mRNAs were detected using RT-PCR, and after 24 h, at which time point the morphology was analyzed by immunofluorescence.

QUANTITATIVE REAL-TIME PCR

Frozen murine LV tissue was pulverized using a pebble mill instrument (Retsch, MM400) before transfer to TRIzol lysis solution to isolate the total RNA from each group. The RNA quality was determined using a NanoDrop 2000C spectrophotometer (Thermo). The RNA was used for further analysis if the OD260/OD280 ratio was within the range 1.9–2.1 and the OD260/230 ratio was greater than two. Reverse transcription reactions were performed using the RT kit (Roche). Primers were used to determine the gene expression of atrial natriuretic peptide (ANP), B-type natriuretic peptide (BNP), β-myosin heavy chain (β-MHC), α-actin (Acta1), procollagen type Iα1 (Col1α1), procollagen type III α1 (Col3α1), fibronectin, transforming growth factor beta 1 (TGF-β1), transforming growth factor beta 2 (TGF-β2), and connective tissue growth factor (CTGF). The relative expression levels of those mRNA were calculated using a comparative method with GAPDH.

WESTERN BLOT ANALYSIS

Frozen murine LV tissue was pulverized in a pebble mill instrument before being transferred to a lysis buffer containing PMSF, NaF, Na3VO4, complete, PhosSTOP, EDTA, and so on. The LV tissue or cells were homogenized using an ultrasound wave cell disruption instrument XL-2000 (Misonix) and centrifuged at $12000 \times g$ for 1 min at 4°C. The supernatants were collected and stored at −80°C. The protein concentrations were measured for each group using the BCA Protein Assay Kit (Thermo), according to the manufacturer's protocol. The tissue or cell extracts were analyzed on 4–10% SDS/PAGE and blotted onto PVDF membranes. The membranes were blocked in 5% non-fat dry milk in Tris-buffered saline with Tween-20 (TBST) for 2 h at room temperature. After washing three times for 5 min each in TBST buffer, the membranes were incubated with primary antibodies (SRF, Santa Cruz, sc-13029) by gentle rocking overnight at 4°C. The secondary antibodies were added and incubated with gentle rocking for 45 min at room temperature before the membranes were washed, as previously described. GAPDH was used as a loading control to determine the protein concentration.

STATISTICAL ANALYSIS

All of the results were derived from 10 to 15 animals in each group, are expressed as the means ± SE, and were analyzed in SPSS13.0. All of the data were tested for normality before comparisons between groups were performed. Post hoc analyses were performed using one-way ANOVA with LSD test or Tamhane's T2 test to compare controls and various treatments, and values of $P < 0.05$ were considered to be statistically significant.

RESULTS

GENERATION AND CHARACTERIZATION OF MIR-150 TRANSGENIC MICE

To determine the functional consequences of miR-150 overexpression in adult hearts in response to pressure overload, we generated a miR-150 transgenic (TG) mouse model using a cardiac-specific promoter. Four independent transgenic lines were initially generated. The successful overexpression of miR-150 in the TG hearts was confirmed by PCR analysis. The line that expressed the highest levels of miR-150 in the heart was selected for our experiments. Under basal conditions, miR-150 transgenic mice exhibited no pathological alterations in ventricular chamber dimensions, ventricular wall thicknesses, left ventricular ejection fraction, LVFS, HW/BW, or LW/BW. Further histological analysis also suggested a lack of gross morphological alterations or fibrosis (data not shown). Thus, miR-150 plays a negligible role in cardiac structure and function under basal conditions.

CARDIAC-SPECIFIC OVEREXPRESSION OF MIR-150 ATTENUATES CARDIAC HYPERTROPHY AND CARDIAC DYSFUNCTION

To investigate the role of miR-150 in biomechanical stress in the heart, TG mice and WT littermates were subjected to AB surgery or sham operation. Cardiac morphology and function were examined after 8 weeks of surgery. The survival rate in the TG group was increased by 25% compared with that of the WT group after 8 weeks of AB (100% vs. 75%). These TG mice exhibited significant attenuation of hypertrophy compared with the WT littermates, as evidenced by the HW/BW and LW/BW ratios as well as the significantly lower CSA in the TG mice compared with that in the WT mice (Fig. 1A). No significant differences were observed in the sham-operated TG and WT mice. The transgene also also inhibited cardiac dilation, wall thickness, and dysfunction, as evidenced by improvements in echocardiographic measurements (Fig. 1B). The gross heart morphology and HE staining further confirmed the inhibitory effect of miR-150 on cardiac hypertrophy after AB (Fig. 1C). We further compared the expression level of several cardiac hypertrophic markers in TG and WT mice after 8 weeks of AB, including ANP, BNP, β-MHC, and Acta 1. Our results revealed that the AB-induced upregulation of hypertrophic markers was significantly reduced in TG mice (Fig. 1D). These results indicate that forced miR-150 expression in the heart attenuates cardiac hypertrophic and cardiac dysfunction after AB.

LOSS OF FUNCTION OF MIR-150 PROMOTES CARDIAC HYPERTROPHY AND CARDIAC DYSFUNCTION

To further test the role of endogenous miR-150 in cardiac hypertrophy, we used two miR-150 loss-of-function approaches. In the first approach, we used miR-150 knockout mice (i.e., KO mice). In the second approach, we infused antagomiR-150 into WT mice to knock down endogenous miR-150 (i.e., AM mice). Next, we applied AB to these animals and analyzed the cardiac morphology and function after 4 weeks of AB. The survival rates in the KO group and AM group exhibited a decreased trend compared with the control groups after 4 weeks of AB (82.4% vs. 85.7%; 73.3% vs. 83.3%, respectively). Both the KO mice and AM mice demonstrated a significant exacerbation of hypertrophy after 4 weeks of AB compared with WT mice or saline-treated mice, as determined by the ratios of HW/BW, LW/BW, and CSA (Fig. 2A and Fig. 3A). The KO mice and AM mice also exhibited deteriorated cardiac hypertrophy and dysfunction as determined by echocardiographic measurements (Fig. 2B and Fig. 3B). The gross heart morphology and HE staining further confirmed that miR-150 promoted cardiac remodeling after AB (Fig. 2C and Fig. 3C). Subsequent analyses of the mRNA levels of the hypertrophic markers ANP, BNP, β-MHC, and Acta 1 revealed that the induction of hypertrophic markers was significantly increased in both the KO mice and AM mice (Fig. 2D and Fig. 3D). These results suggest that miR-150 knockdown promotes cardiac hypertrophy and deteriorates impaired cardiac function after pressure overload.

EFFECT OF MIR-150 ON HYPERTROPHY IN VITRO

To further confirm the effect of miR-150 on cardiac hypertrophy, we performed gain- and loss-of-function studies in an in vitro model of cellular growth using cultured H9C2 cells. After treatment with miR-150 mimics or antagomiR-150, the cells were exposed to 1 μM Ang II. Our results demonstrated that treatment with miR-150 mimics significantly attenuated the increase in cell surface area induced by Ang II treatment, whereas antagomiR-150 treatment promoted these effects of Ang II (Fig. 4). These findings indicate that miR-150 inhibits cardiac hypertrophy in vitro.

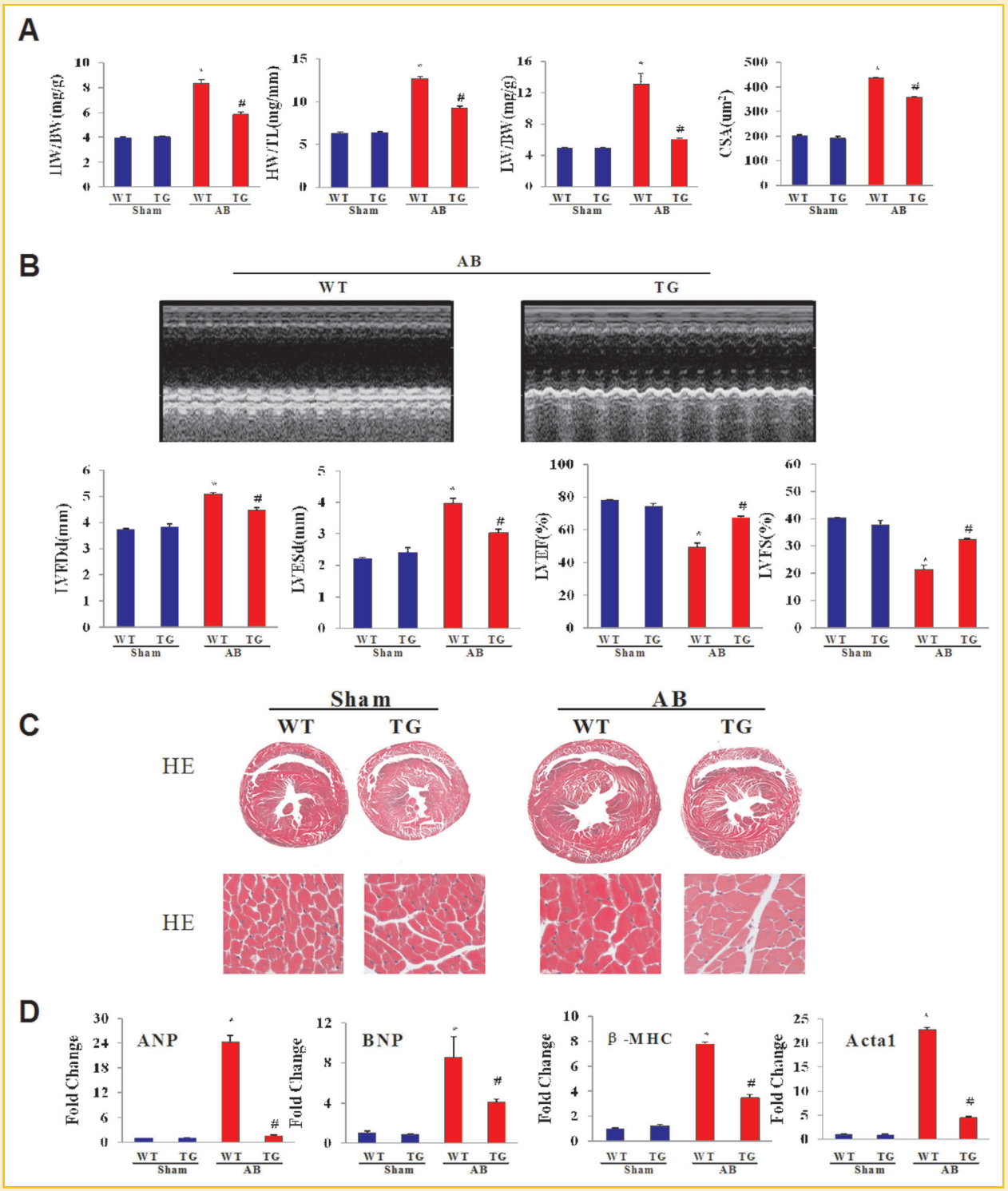

Fig. 1. The effect of miR-150 on cardiac hypertrophy in TG mice in vivo. (A) Statistical results for the HW/BW, HW/TL, and LW/BW ratios and the myocyte CSA (n = 100 + cells) 8 weeks after AB in WT and TG mice (n = 11–15). (B) Statistical results for the LVEDD, LVESD, LVEF, and LVFS in WT and TG mice (n = 5–7). (C) Gross hearts morphology and HE staining at 8 weeks after AB in WT and TG mice (n = 5). (D) The expression of hypertrophic markers induced by AB was determined using real-time PCR analysis in WT and TG mice (n = 4). $^{*}P < 0.05$ for WT/sham; $^{\#}P < 0.05$ for WT/AB.

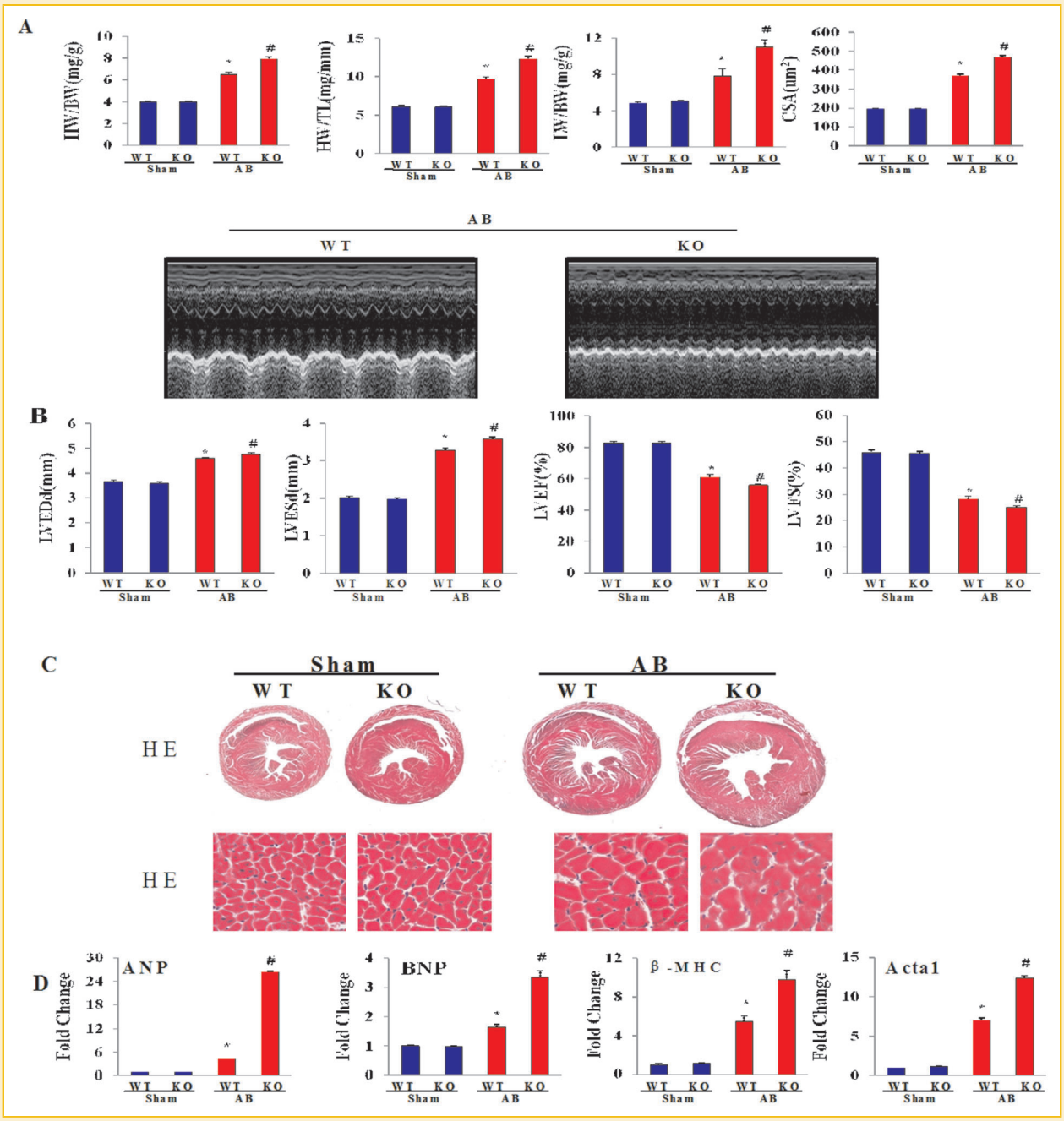

Fig. 2. The effect of miR-150 on cardiac hypertrophy in KO mice in vivo. (A) Statistical results for the HW/BW, HW/TL, and LW/BW ratios and the myocyte CSA (n = 100 cells per group) 4 weeks after AB in WT and KO mice (n = 11–14). (B) Statistical results for the LVEDD, LVESD, LVEF, and LVFS in WT and KO mice (n = 5–9). (C) Gross hearts morphology and HE staining at 4 weeks after AB in WT and KO mice (n = 5). (D) The expression of hypertrophic markers induced by AB was determined using real-time PCR analysis in WT and KO mice (n = 4). $^{*}P < 0.05$ for WT/sham; $^{\#}P < 0.05$ for WT/AB.

EFFECT OF MIR-150 ON SRF PROTEIN EXPRESSION

Using a miR target prediction algorithm (TargetScan 5.2), we revealed that miR-150 had 118 potential targets. Of these potential targets, SRF has been reported to play an important role in the regulation of genes responsible for cardiac structure and function. To ascertain whether miR-150 inhibits the hypertrophic response by regulating SRF expression in the heart, we examined SRF protein expression using Western blot analysis. We discovered that the SRF protein levels were significantly increased in the hearts of WT mice subjected to AB. However, the increased level of SRF protein was significantly attenuated in the hearts of TG mice (Fig. 5A). To further confirm the effect of miR-150 on SRF protein expression, we applied AB to KO mice and AM mice. After 4 weeks, AB caused a significant increase in SRF protein levels in both KO

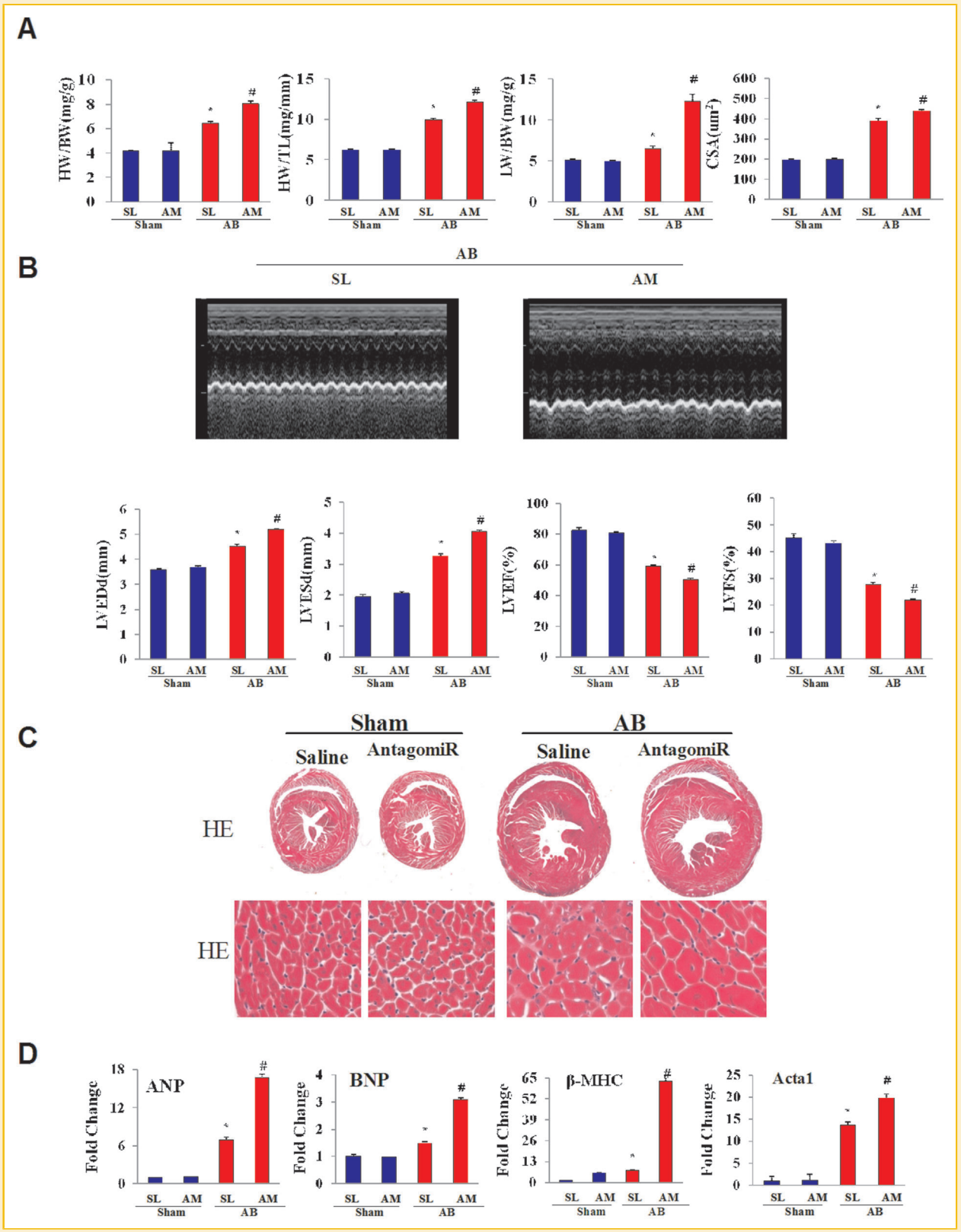

Fig. 3. The effect of miR-150 on cardiac hypertrophy in antagomiR-150-treated (AM) mice in vivo. (A) Statistical results for the HW/BW, HW/TL, and LW/BW ratios and the myocyte CSA (n = 100 cells per group) 4 weeks after AB in saline (SL) and AM mice (n = 11–15). (B) Statistical results for the LVEDD, LVESD, LVEF, and LVFS in AM and SL mice (n = 6–7). (C) Gross hearts morphology and HE staining at 4 weeks after AB in SL and AM mice (n = 5). (D) The expression of hypertrophic markers induced by AB was determined using real-time PCR analysis in SL and AM mice (n = 4). $^{*}P < 0.05$ for SL/sham; $^{\#}P < 0.05$ for SL/AB.

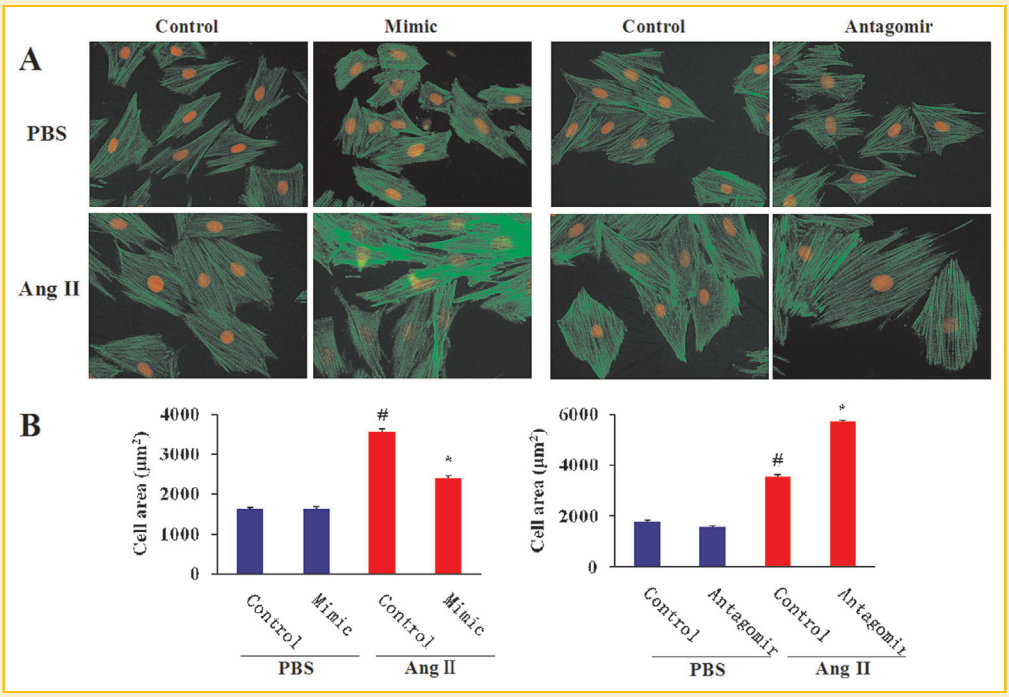

Fig. 4. The effect of miR-150 on hypertrophy in vitro. (A) Representative images of cultured H9C2 cells treated with miR-150 mimics or antagomiR-150 in response to Ang II. (B) Analysis of cell area in the indicated groups. $^{\#}P < 0.05$ for control/PBS ; $^{*}P < 0.05$ for control/Ang II.

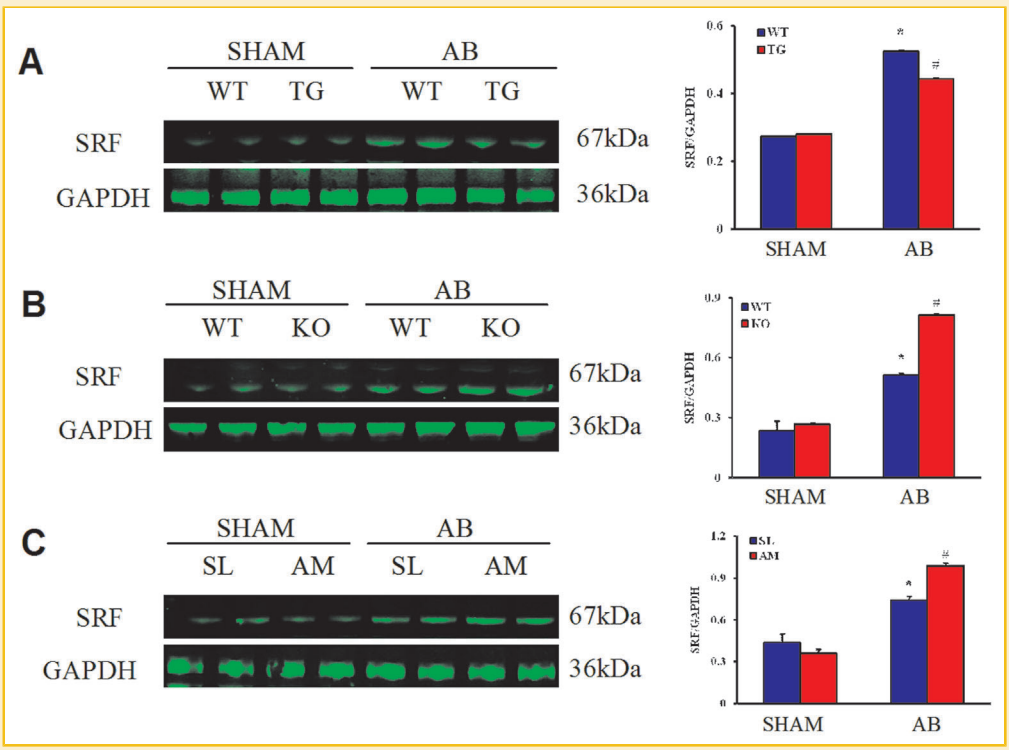

Fig. 5. The effect of miR-150 on SRF expression in vivo. (A) Left: Representative blots of SRF expression at 8 weeks after AB surgery in WT mice and TG mice. Right: Quantitative results (n = 4). (B) Left: Representative blots of SRF expression at 4 weeks after AB surgery in WT mice and KO mice. Right: Quantitative results (n = 4). (C) Left: Representative blots of SRF expression at 4 weeks after AB surgery in saline (SL) mice and antagomiR-150-treated (AM) mice. Right: Quantitative results (n = 4). Reproducible results were obtained in three independent experiments. $^{*}P < 0.05$ for WT/sham or SL/sham; $^{\#}P < 0.05$ for WT/AB or SL/AB.

mice and AM mice compared with WT mice or saline-treated mice (Fig. 5B and Fig. 5C). Collectively, these data indicate that miR-150 negatively regulates SRF protein levels in the heart.

EFFECT OF MIR-150 ON FIBROSIS

To examine the role of miR-150 in cardiac fibrosis, heart sections were stained with PSR to detect fibrosis. Marked perivascular and interstitial fibrosis were detected in the WT mice subjected to AB; however, this staining was remarkably reduced in TG hearts (Fig. 6A). Subsequent quantitative analysis also indicated reduced collagen volume in the hearts of TG mice compared with WT mice (Fig. 6B). Reduced fibrosis in TG mice may represent increased collagen degradation or decreased collagen synthesis in response to hypertrophic stimuli. We therefore examined the mRNA levels of known mediators of fibrosis, including Col1α1, Col3α1, fibronectin, TGF-β1, TGF-β2, and CTGF. The results indicated that Col1α1, Col3α1, fibronectin, TGF-β1, TGF-β2, and CTGF were significantly lower in TG mice than in WT mice in response to AB, suggesting a reduced fibrotic response in TG mice (Fig. 6C). To further confirm the role of miR-150 in cardiac fibrosis, KO mice and AM mice were employed to determine whether the loss of function of miR-150 promotes fibrosis. Further studies suggested that the perivascular and interstitial fibrosis induced by AB was exacerbated by miR-150 knockdown. Subsequent analysis of the mRNA expression of markers for fibrosis also suggested a greater fibrotic response in both KO mice and AM mice compared with WT mice (Fig. 7 and Fig. 8). Taken together, these data indicate that miR-150 reduces the extent of cardiac fibrosis in response to pressure overload.

DISCUSSION

Recently, several studies reported the miR expression profile of hypertrophic hearts from animal models and human patients. However, the role of any specific miR in the development of cardiac hypertrophy is still not completely elucidated. We therefore, for the first time, investigated the functional consequences of miR-150 in vivo and in vitro using gain-of-function and loss-of-function approaches. We were excited to discover that the forced cardiac expression of miR-150 protects against maladaptive hypertrophy and fibrosis in response to chronic pressure overload, whereas the loss of miR-150 function by genetic knockdown or antagomiR approaches elicited the opposite effect. These novel findings clearly demonstrate that miR-150 is critically important in protecting the heart from hypertrophic stimuli. To our knowledge, these data provide the first direct evidence that miR-150 plays a crucial role in the regulation of cardiac hypertrophy and may be a new, useful intervention target for cardiac hypertrophy.

The mechanism by which miR-150 mediates its antihypertrophic effects remains elusive. Using a miR target prediction algorithm, we discovered that SRF is a potential target for

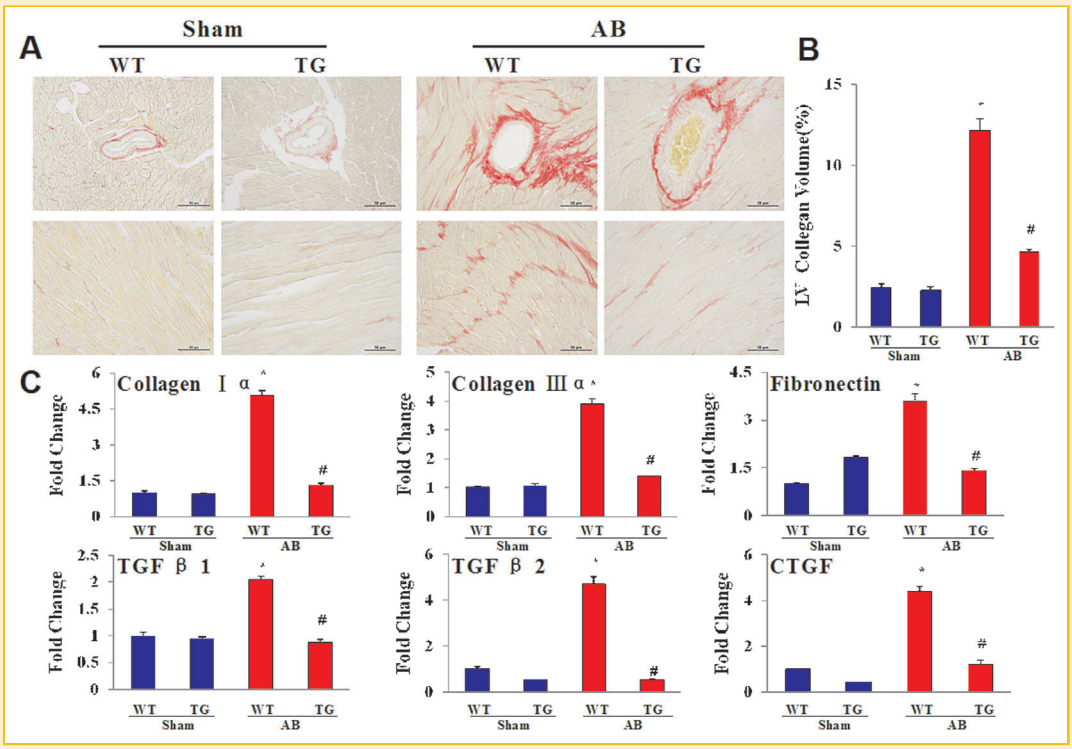

Fig. 6. The effect of miR-150 on cardiac fibrosis in TG mice in vivo. (A) PSR staining of histological sections of the LV was performed on the indicated groups 8 weeks after AB (n = 5). (B) The fibrotic areas of the histological sections were quantified using an image analyzing system (n = 5). (C) Real-time PCR analyses of Col1α1, Col3α1, fibronectin, TGF-β1, TGF-β2, and CTGF were performed to determine the mRNA expression levels in indicated mice (n = 4). $^{*}P < 0.05$ for WT/sham; $^{\#}P < 0.05$ for WT/AB.

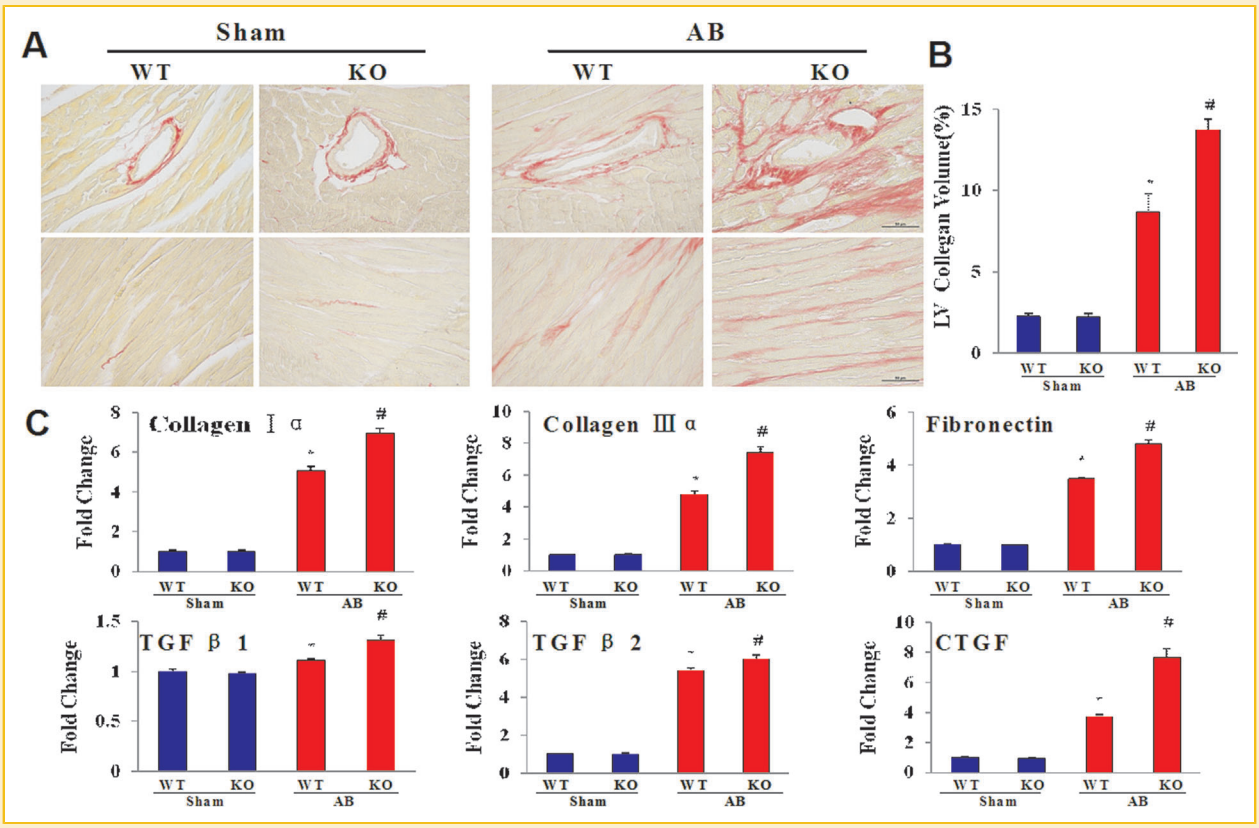

Fig. 7. The effect of miR-150 on cardiac fibrosis in KO mice in vivo. (A) PSR staining of histological sections of the LV was performed on the indicated groups 4 weeks after AB ($n = 5$). (B) The fibrotic areas of the histological sections were quantified using an image analyzing system ($n = 5$). (C) Real-time PCR analyses of Col1α1, Col3α1, fibronectin, TGF-β1, TGF-β2, and CTGF were performed to determine the mRNA expression levels in the indicated mice ($n = 4$). $^{*}P < 0.05$ for WT/sham; $^{\#}P < 0.05$ for WT/AB.

miR-150. SRF has been reported to play an important role in the regulation of genes responsible for cardiac structure and function [Balza and Misra, 2006]. SRF is a member of the MADS box family of transcription factors that has been implicated in the regulation of a number of cardiac muscle genes [McDonald et al., 2006]. In isolated cardiomyocytes, SRF is required for the induction of atrial naturetic factor (ANF), BNP, Acta 1, α-MHC, and β-MHC, suggesting that SRF is critical for the regulation and induction of genes associated with the progression of pathologic cardiac hypertrophy [Nelson et al., 2005]. Transgenic mice with moderate cardiac-specific overexpression of the human SRF gene manifested significant cardiac hypertrophy and premature death [Zhang et al., 2001]. Conversely, the heart-specific deletion of SRF in the embryo resulted in lethal cardiac defects [Parlakian et al., 2004]. Disrupting the SRF gene in adult heart induced a rapid progression to dilated cardiomyopathy [Parlakian et al., 2005]. These findings suggest that SRF is necessary for normal cardiac development and the maintenance of normal function in the heart. Both the loss and gain of SRF function are extremely detrimental to the heart. In our present study, we determined that AB induced a significant increase in SRF protein expression. We also discovered that cardiac-specific overexpression of miR-150 caused a significant decrease in the level of the SRF protein, whereas the deletion or inhibition of miR-150 induced the overexpression of SRF, suggesting that SRF is involved in miR-150 mediated anti-hypertrophic effect. However, as miR-150 may target multiple target genes simultaneously, it should be noted that our results demonstrate that SRF is an important, but possibly not the only, target of miR-150 in hypertrophic hearts.

Presently, more than 10 miRs have been identified as regulators of cardiac hypertrophy [Da Costa Martins and De Windt, 2012]. Among these RNAs, certain miRs have been demonstrated to be anti-hypertrophic, whereas others are pro-hypertrophic. Furthermore, it appears that different miRs have distinct mechanisms in regulating cardiac hypertrophy. For example, decreased expression of miR-133 contributed to cardiac hypertrophy by regulating the GDP-GTP exchange protein RhoA, transduction kinase Cdc42, and nuclear factor Nelf-A/WHSC2, whereas the upregulated expression of miR-23a promoted cardiac hypertrophy by targeting the muscle-specific ring finger protein 1(MuRF1) [Carè et al., 2007; Lin et al., 2009]. These studies implied that cardiac hypertrophy is a complex pathological process, and miRs may be involved in many aspects of hypertrophy. Interesting, a recent study reported that cardiac-specific overexpression of SRF downregulated miR-1 and miR-133a and upregulated miR-21, all of

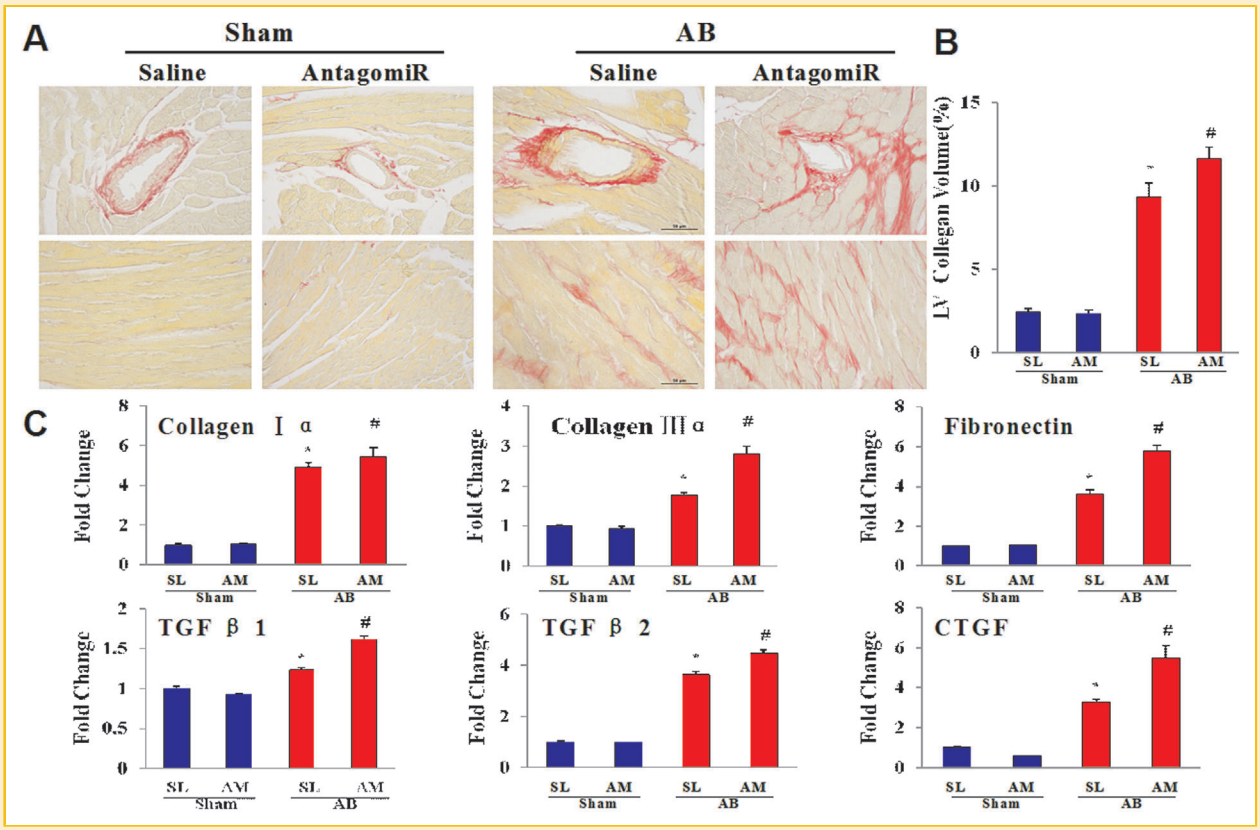

Fig. 8. The effect of miR-150 on cardiac fibrosis in antagomiR-150-treated (AM) mice in vivo. (A) PSR staining of histological sections of the LV was performed on the indicated groups 4 weeks after AB (n = 5). (B) The fibrotic areas of the histological sections were quantified using an image analyzing system (n = 5). (C) Real-time PCR analyses of Col1α1, Col3α1, fibronectin, TGF-β1, TGF-β2, and CTGF were performed to determine the mRNA expression levels in the indicated mice (n = 4). $^{*}P < 0.05$ for saline (SL)/sham; $^{\#}P < 0.05$ for SL/AB.

which are typically dysregulated during cardiac hypertrophy [Zhang et al., 2011]. Therefore, there may be interactions between miRs in the complex regulatory network governing cardiac hypertrophy. The overexpression of miR-150 in our study downregulated SRF, which may secondarily affect other miRs related to the development of cardiac hypertrophy. However, this possibility will need to be specifically investigated in future studies.

Fibrosis is a classic feature of pathological hypertrophy [Bian et al., 2014; Liu et al., 2014]. Another major finding of this study is that miR-150 inhibits cardiac fibrosis in vivo. To our knowledge, our study reports for the first time that miR-150 inhibits cardiac fibrosis in response to pressure overload. A recent study indicated that SRF plays a critical role in myofibroblast differentiation and fibrosis induced by TGF-β [Sandbo et al., 2009]. TGF-β stimulation results in the activation of Rho-Rho-kinase signaling, reorganization of the actin cytoskeleton, and nuclear translocation of SRF coactivators, thereby promoting the SRF-dependent transcription of genes encoding extracellular matrix components [Kuwahara et al., 2007; Small et al., 2010]. Histological examination revealed significant collagen deposition and fibrosis in the hearts from transgenic mice with cardiac-specific overexpression of SRF [Zhang et al., 2001]. The genetic deletion of SRF coactivators in mice reduced cardiac fibrosis in response to myocardial infarction or Ang II treatment [Small et al., 2010]. These findings suggest that the inhibitory effect of miR-150 on fibrosis in the present study may be attributed to its negative regulation of SRF, at least in part.

In conclusion, our study identified the crucial role of miR-150 in protecting against cardiac hypertrophy and fibrosis in response to pressure overload through the downregulation of SRF. These observations may have significant implications for developing a novel therapeutic target for the treatment or prevention of cardiac hypertrophy.

REFERENCES

Aurora AB, Mahmoud AI, Luo X, Johnson BA, van Rooij E, Matsuzaki S, Humphries KM, Hill JA, Bassel-Duby R, Sadek HA, Olson EN. 2012. MicroRNA-214 protects the mouse heart from ischemic injury by controlling Ca^{2+} overload and cell death. J Clin Invest 122:1222–1232.

Balza RO Jr, Misra RP. 2006. Role of the serum response factor in regulating contractile apparatus gene expression and sarcomeric integrity in cardiomyocytes. J Biol Chem 281:6498–6510.

Bian Z, Dai J, Hiroyasu N, Guan H, Yuan Y, Gan L, Zhou H, Zong J, Zhang Y, Li F, Yan L, Shen D, Li H, Tang Q. 2014. Disruption of tumor necrosis factor receptor associated factor 5 exacerbates pressure overload cardiac hypertrophy and fibrosis. J Cell Biochem 115:349–358.

Carè A, Catalucci D, Felicetti F, Bonci D, Addario A, Gallo P, Bang ML, Segnalini P, Gu Y, Dalton ND, Elia L, Latronico MV, Hùydal M, Autore C, Russo MA, Dorn GW 2nd, Ellingsen O, Ruiz-Lozano P, Peterson KL, Croce CM, Peschle C, Condorelli G. 2007. MicroRNA-133 controls cardiac hypertrophy. Nat Med 13:613–618.

Da Costa Martins PA, De Windt LJ. 2012. MicroRNAs in control of cardiac hypertrophy. Cardiovasc Res 93:563–572.

Fulci V, Chiaretti S, Goldoni M, Azzalin G, Carucci N, Tavolaro S, Castellano L, Magrelli A, Citarella F, Messina M, Maggio R, Peragine N, Santangelo S, Mauro FR, Landgraf P, Tuschl T, Weir DB, Chien M, Russo JJ, Ju J, Sheridan R, Sander C, Zavolan M, Guarini A, Foà R, Macino G. 2007. Quantitative technologies establish a novel microRNA profile of chronic lymphocytic leukemia. Blood 109:4944–4951.

Jing Q, Huang S, Guth S, Zarubin T, Motoyama A, Chen J, Di Padova F, Lin SC, Gram H, Han J. 2005. Involvement of microRNA in AU-rich element-mediated mRNA instability. Cell 120:623–634.

Kuwahara K, Teg Pipes GC, McAnally J, Richardson JA, Hill JA, Bassel-Duby R, Olson EN. 2007. Modulation of adverse cardiac remodeling by STARS, a mediator of MEF2 signaling and SRF activity. J Clin Invest 117:1324–1334.

Li H, He C, Feng J, Zhang Y, Tang Q, Bian Z, Bai X, Zhou H, Jiang H, Heximer SP, Qin M, Huang H, Liu PP, Huang C. 2010. Regulator of G protein signaling 5 protects against cardiac hypertrophy and fibrosis during biomechanical stress of pressure overload. Proc Natl Acad Sci USA 107:13818–13823.

Lin Z, Murtaza I, Wang K, Jiao J, Gao J, Li PF. 2009. MiR-23a functions downstream of NFATc3 to regulate cardiac hypertrophy. Proc Natl Acad Sci USA 106:12103–12108.

Liu Y, Huang H, Zhang Y, Zhu XY, Zhang R, Guan LH, Tang Q, Jiang H, Huang C. 2014. Regulator of G protein signaling 3 protects against cardiac hypertrophy in mice. J Cell Biochem 115:977–986.

Lorell BH, Carabello BA. 2000. Left ventricular hypertrophy: Pathogenesis, detection, and prognosis. Circulation 102:470–479.

McDonald OG, Wamhoff BR, Hoofnagle MH, Owens GK. 2006. Control of SRF binding to CArG box chromatin regulates smooth muscle gene expression in vivo. J Clin Invest 116:36–48.

Montgomery RL, Hullinger TG, Semus HM, Dickinson BA, Seto AG, Lynch JM, Stack C, Latimer PA, Olson EN, van Rooij E. 2011. Therapeutic inhibition of miR-208a improves cardiac function and survival during heart failure. Circulation 124:1537–1547.

Nelson TJ, Balza R Jr, Xiao Q, Misra RP. 2005. SRF-dependent gene expression in isolated cardiomyocytes: Regulation of genes involved in cardiac hypertrophy. J Mol Cell Cardiol 39:479–489.

Parlakian A, Charvet C, Escoubet B, Mericskay M, Molkentin JD, Gary-Bobo G, De Windt LJ, Ludosky MA, Paulin D, Daegelen D, Tuil D, Li Z. 2005. Temporally controlled onset of dilated cardiomyopathy through disruption of the SRF gene in adult heart. Circulation 112:2930–2939.

Parlakian A, Tuil D, Hamard G, Tavernier G, Hentzen D, Concordet JP, Paulin D, Li Z, Daegelen D. 2004. Targeted inactivation of serum response factor in the developing heart results in myocardial defects and embryonic lethality. Mol Cell Biol 24:5281–5289.

Ruilope LM, Schmieder RE. 2008. Left ventricular hypertrophy and clinical outcomes in hypertensive patients. Am J Hypertens 21:500–508.

Sandbo N, Kregel S, Taurin S, Bhorade S, Dulin NO. 2009. Critical role of serum response factor in pulmonary myofibroblast differentiation induced by TGF-beta. Am J Respir Cell Mol Biol 41:332–338.

Sayed D, Hong C, Chen IY, Lypowy J, Abdellatif M. 2007. MicroRNAs play an essential role in the development of cardiac hypertrophy. Circ Res 100:416–424.

Small EM, Thatcher JE, Sutherland LB, Kinoshita H, Gerard RD, Richardson JA, Dimaio JM, Sadek H, Kuwahara K, Olson EN. 2010. Myocardin-related transcription factor-a controls myofibroblast activation and fibrosis in response to myocardial infarction. Circ Res 107:294–304.

van Rooij E, Sutherland LB, Liu N, Williams AH, McAnally J, Gerard RD, Richardson JA, Olson EN. 2006. A signature pattern of stress-responsive microRNAs that can evoke cardiac hypertrophy and heart failure. Proc Natl Acad Sci USA 103:18255–18260.

Vasilescu C, Rossi S, Shimizu M, Tudor S, Veronese A, Ferracin M, Nicoloso MS, Barbarotto E, Popa M, Stanciulea O, Fernandez MH, Tulbure D, Bueso-Ramos CE, Negrini M, Calin GA. 2009. MicroRNA fingerprints identify miR-150 as a plasma prognostic marker in patients with sepsis. PLoS One 4:e7405.

Wang X, Zhang X, Ren XP, Chen J, Liu H, Yang J, Medvedovic M, Hu Z, Fan GC. 2010. MicroRNA-494 targeting both proapoptotic and antiapoptotic proteins protects against ischemia/reperfusion-induced cardiac injury. Circulation 122:1308–1318.

Watanabe A, Tagawa H, Yamashita J, Teshima K, Nara M, Iwamoto K, Kume M, Kameoka Y, Takahashi N, Nakagawa T, Shimizu N, Sawada K. 2011. The role of microRNA-150 as a tumor suppressor in malignant lymphoma. Leukemia 25:1324–1334.

Wu L, Fan J, Belasco JG. 2006. MicroRNAs direct rapid deadenylation of mRNA. Proc Natl Acad Sci USA 103:4034–4039.

Xiao C, Calado DP, Galler G, Thai TH, Patterson HC, Wang J, Rajewsky N, Bender TP, Rajewsky K. 2007. MiR-150 controls B cell differentiation by targeting the transcription factor c-Myb. Cell 131:146–159.

Yang B, Lin H, Xiao J, Lu Y, Luo X, Li B, Zhang Y, Xu C, Bai Y, Wang H, Chen G, Wang Z. 2007. The muscle-specific microRNA miR-1 regulates cardiac arrhythmogenic potential by targeting GJA1 and KCNJ2. Nat Med 13: 486–491.

Zhang X, Azhar G, Chai J, Sheridan P, Nagano K, Brown T, Yang J, Khrapko K, Borras AM, Lawitts J, Misra RP, Wei JY. 2001. Cardiomyopathy in transgenic mice with cardiac-specific overexpression of serum response factor. Am J Physiol Heart Circ Physiol 280:H1782–H1792.

Zhang X, Azhar G, Helms SA, Wei JY. 2011. Regulation of cardiac microRNAs by serum response factor. J Biomed Sci 18:15.

Zhou L, Qi X, Potashkin JA, Abdul-Karim FW, Gorodeski GI. 2008. MicroRNAs miR-186 and miR-150 down-regulate expression of the pro-apoptotic purinergic P2×7 receptor by activation of instability sites at the 3′-untranslated region of the gene that decrease steady-state levels of the transcript. J Biol Chem 283:28274–28286.

Zong J, Zhang DP, Zhou H, Bian ZY, Deng W, Dai J, Yuan Y, Gan HW, Guo HP, Tang QZ. 2013. Baicalein protects against cardiac hypertrophy through blocking MEK-ERK1/2 signaling. J Cell Biochem 114: 1058–1065.

SUPPORTING INFORMATION

Additional supporting information may be found in the online version of this article at the publisher's web-site.